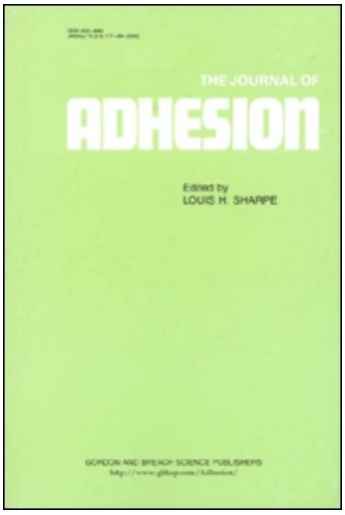

The Journal of Adhesion
Publication details, including instructions for authors and subscription information:
http://www.informaworld.com/smpp/title~content=t713453635

Analysis and Design of Adhesive Mechanical Characterization Test Specimens

W. J. Renton

To cite this Article Renton, W. J.(1979) 'Analysis and Design of Adhesive Mechanical Characterization Test Specimens', The Journal of Adhesion, 10: 2, 139 — 155
To link to this Article: DOI: 10.1080/00218467908544620
URL: http://dx.doi.org/10.1080/00218467908544620

J. Adhesion, 1979, Vol. 10, pp. 139–155
0021-8464/79/1001-0139 $04.50/0

Printed in Scotland

Analysis and Design of Adhesive Mechanical Characterization Test Specimens

W. J. RENTON

Vought Corporation, P.O. Box 6144, Dallas, Texas 75222, U.S.A.

(*Received January 24, 1978; in final form February 10, 1979*)

To design bonded structures efficiently, the "in situ" mechanical properties of the adhesive must be known. Yet, the difficulty associated with accurately measuring the subject mechanical properties in tension and tension plus shear has plagued the engineering community for years. This paper presents a detailed analysis which for the first time accounts for adherend elasticity of two test specimen geometries that may be used to obtain the desired adhesive properties, namely a rectangular and circular scarf (butt) joint. To obtain accurate properties, an optimum specimen geometry must be defined. This optimum geometry is defined by the ratio (aspect ratio) of span (2a) *vs.* adhesive thickness (2) for the rectangular geometry and by the diameter (2r) *vs.* adhesive thickness ratio for the circular geometry. In both instances, an aspect ratio of forty or larger is required to obtain a nearly uniform adhesive tensile and/or shear stress magnitude over 90–95% of the adhesive cross section, thereby minimizing the free edge effect. Such a geometry is mandatory if meaningful adhesive property data are to be obtained for design purposes.

INTRODUCTION

It has been the usual practice to utilize the bulk mechanical properties of adhesives in the analysis and design of metal or non-metal bonded joints. This is erroneous as the adhesive system in most structural joints is of the order of thousandths of an inch in thickness. Moreover, Zabora *et al.*,[1] and Hughes and Rutherford[2] point out that thin film adhesive properties are, in general, significantly different than those of the bulk adhesive. This is especially true in relation to the surface chemistry at the adhesive–adherend interface (adhesive–air interface for bulk specimens), the residual strains "locked in" a bonded joint during an elevated temperature cure and the

constraining Poisson's effect of the stiffer adherend on the relatively soft adhesive (tension mode).

Various specimens have been looked at in an attempt to obtain the tensile and/or biaxial properties of adhesives. Bulk tensile specimens[3-5] have included the dog bone, bulk thin-walled tube and bulk solid rod. The latter two specimens suffer from fabrication difficulties and a relatively high cost per specimen. All three specimens, while providing quantitative results, are unable to duplicate the adhesive-adherend factors detailed above.

The scarf joint and napkin-ring test specimens[1, 2, 7-21] can alleviate these problems and provide a controllable biaxial (i.e., tension plus shear) stress state within the thin adhesive bondline. Most recently, the napkin-ring specimen has been used to obtain shear and tensile properties.[2, 14, 16, 22] The specimen itself suffers from being difficult to fabricate to prescribed adhesive thicknesses. Additionally, the cost per test item is quite high, inspectability using non-destructive (NDI) means is difficult and control of the biaxial load into the specimen requires extreme care.

An alternate approach, namely the scarf joint, has been proposed[17, 18] as a viable specimen with which to obtain the effective thin film tensile or biaxial properties of adhesives. While being relatively easy to fabricate,[23] and of modest cost,[4] it too suffers somewhat from a bondline inspectability problem. However, newer NDI techniques, namely Neutron Radiography, offer a realistic approach to resolving this problem.[23] Therefore, this specimen can provide data that are readily usable in today's numerous analysis methods that determine stresses and deformations in both the adhesive and adherends of bonded joints. Further, the trends associated with cogent variables such as adhesive thickness, surface roughness, temperature, moisture and strain rate can be obtained through consistent use of this test specimen.

This paper looks in depth at the proposed scarf (butt) joint test specimen in an attempt to analytically justify its usefulness in obtaining realistic adhesive tensile and biaxial properties. In doing this, an analytical model has been formulated which accounts for the adherends' elasticity and serves to define the geometrical constraints within which realistic static and viscoelastic adhesive mechanical property data can be obtained. Moreover, verification of the analytical model's correctness is shown for the limiting condition of infinitely rigid adherends, and the parameters that are most influential in the design of an optimum test specimen are specified.

ANALYTICAL APPROACH

Examination, in a realistic manner, of the stress (strain) state in an adhesively bonded scarf (butt) joint configuration, requires that a specific closed form

analytical model be derived. The analysis presented enables one to determine the optimum specimen dimensions to maximize the uniform stress (strain) region in the adhesive, thereby minimizing disruptive edge effects for a particular test geometry. Employing these optimal test specimens, one may obtain accurate adhesive mechanical property data and account for the fact that the apparent adhesive modulus measured during an actual test is a known percentage of the true uniaxial adhesive modulus. This relationship is a function of adhesive and adherend properties and specimen geometry. The mechanical property data obtained using these specimens will be the subject of a future paper.

Several attempts to analyze the scarf[17] or butt[3, 25, 26, 28] joint have been made. In all instances, the constraining effect of the stiffer adherend material on the adhesive and the viscoelastic nature of the adhesive were neglected. The ensuing analysis accounts for finite adherend properties and uses as a starting point the analytical model developed in Ref. 3. Both the circular and rectangular scarf joint geometries are looked at. Once the stresses (strains) in the rectangular (circular) scarf joint are defined, it is a simple matter to obtain the stresses (strains) in the butt joint.

A rigorously correct mathematical model for the scarf (butt) joint configuration leads to a mixed boundary value problem that is essentially intractable using a classical elasticity approach. This is primarily due to the discontinuous boundary condition the joint presents at the right angled corner where the adherend surface is appreciably stiffer than the adhesive while the adhesive's surface is free of stress. The ensuing stress singularity is not accounted for within the analysis. Its effect can be quantified using the analytical approach found in Ref. 3. Moreover, its degree of penetration from the adhesive's free surface inward is a function of the specimen's shear modulus and Poisson's ratio. A realistic specimen design ($a \gg \eta$) will restrict the effect of this singularity to within one to two adhesive thicknesses from the adhesive's free surface.

FORMULATION OF THE PROBLEM (RECTANGULAR GEOMETRY)

The rectangular scarf joint geometry and notation are shown in Figure 1a. The joint is assumed to be infinitely long in the z-direction (i.e., $L/a \gg 1$) and is therefore considered to be in a generalized plane strain state. Linear elastic analysis is used with the inclusion of linear viscoelastic effects by means of the "quasi-elastic" approach. The adherend material is assumed to be linearly elastic, isotropic and homogeneous. Its effect on the adhesive is realized through use of the adherend displacement boundary conditions,

while the adhesive is characterized in a linearly viscoelastic manner. It too is assumed to be isotropic and homogeneous. Additional assumptions are that the bond between the adhesive and the adherend is structurally sound, the stresses and displacements vary over the adhesive thickness in a prescribed manner, that adhesive planes originally parallel to the adherend interface remain parallel upon loading and that the adhesive–adherend discontinuity effect is defined by the unknown function $f(s)$.

The adhesive's geometry and notation are shown in Figure 1b. The adhesive half-thickness is taken as unity for simplicity, but without loss of generality.

The adhesive slab is bonded to the two deformable adherends at $n = \pm 1$. The adhesive is loaded in the η-direction by a load ($P \sin \theta$) which increases the adhesive thickness by 2ε and a shear load ($P \cos \theta$). It is desired to determine the state of stress (strain) in the adhesive for this system of external forces.

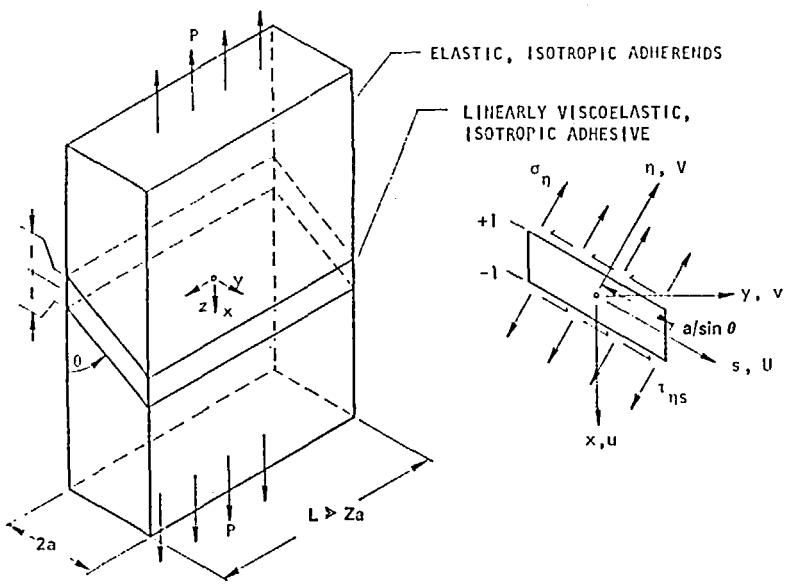

FIGURE 1 Rectangular scarf joint geometry.

ELASTIC ADHEREND BOUNDARY CONDITIONS

The displacement boundary conditions at the adhesive–adherend interface can be ascertained by determining the displacements in a solid homogeneous

linearly elastic, isotropic bar when subjected to a uniform axial tensile stress (σ_x) over its cross-section. The resulting displacements and strains are:

$$u = \frac{\sigma_x x}{\hat{E}} + C_2 y + C_1; \qquad v = \frac{-\hat{\nu}\sigma_x y}{\hat{E}} - C_2 x + C_3; \qquad w = \frac{-\hat{\nu}\sigma_x z}{\hat{E}} + C_4 \quad (1)$$

$$\hat{\varepsilon}_x = \frac{\partial u}{\partial x} = \frac{\sigma_x}{\hat{E}}; \quad \hat{\varepsilon}_y = \frac{\partial v}{\partial y} = \frac{-\hat{\nu}\sigma_x}{\hat{E}}; \quad \hat{\varepsilon}_z = \frac{-\hat{\nu}\sigma_x}{\hat{E}} = \text{const.}; \; \hat{\gamma}_{xy} = \hat{\gamma}_{xz} = \hat{\gamma}_{yz} = 0 \quad (2)$$

The constants $\hat{\nu}$ and $\hat{E}$ are the Poisson's ratio and Young's modulus of the adherend material while, u, v, and w are the displacements in the x, y and z directions, respectively. The constants C_1, C_3 and C_4 define the reference location with respect to the coordinates origin from which all deformation measurements are made. C_1, C_3 and C_4 will be equated to zero.

Lubkin[17] has shown that relative rotation between identical adherends pin loaded at points (A) and (B) is absent. However, it can be shown that the specimen as a whole rotates in the (x–y) plane and that this rotation is given by the (C_2) term in Eq. (1). The rotation it refers to is depicted in Figure 2 and is independent of cross-sectional geometry. It can be directly determined by measuring the rotation of a vertical side of the specimen with a high resolution optical measurement device as the specimen is loaded. Alternately, the rotation can be obtained by measuring the specimen's displacement parallel (U) and perpendicular (V) to the adhesive-adherend interface and using the relationship:

$$C_2 = \frac{V \cos\theta - U \sin\theta}{l/2}$$

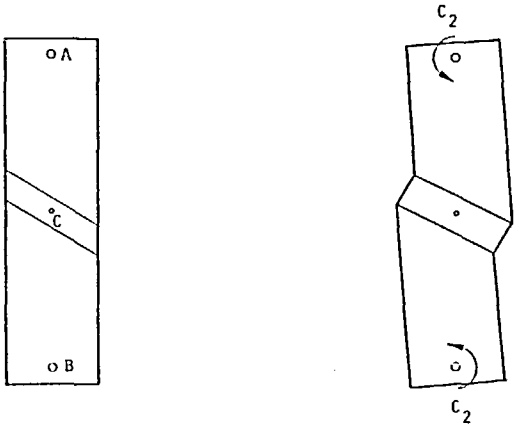

(a) unloaded (b) loaded

FIGURE 2 Rotation of a typical scarf joint.

Moreover, it can be shown, by the use of symmetry arguments, that there is no horizontal movement of the center point (C) and that the deformation across the adhesive thickness from right to left is symmetric. Therefore, the rotation of the upper and lower adherends (C_2) must be in the same direction and does occur about pins (A) and (B).

Let $\hat{U}$ and $\hat{V}$ be the adherend displacements in the (s) and (η) directions, respectively. Then per the well-known transformation of axes formulas:

$$\hat{U} = u\cos\theta + v\sin\theta$$
$$\hat{V} = v\cos\theta - u\sin\theta \tag{3}$$

Similarly, the coordinate transformation from the (x–y) to the (s, η) axes is:

$$x = s\cos\theta - \eta\sin\theta$$
$$y = s\sin\theta + \eta\cos\theta \tag{4}$$

Substitution of Eq. (1) into Eq. (3) and employing the coordinate transformation relations [Eq. (4)], provides the formulas for the adherend displacement functions with reference to the (s, η) axes, namely:

$$\hat{U} = As + B\eta; \qquad \hat{V} = \beta\eta - Ds \tag{5, 6}$$

where:

$$A = \frac{\sigma_x}{\hat{E}}(\cos^2\theta - \hat{\nu}\sin^2\theta); \qquad D = \frac{\sigma_x}{\hat{E}}(1+\hat{\nu})\sin\theta\cos\theta + C_2 \tag{7}$$

$$B = -\frac{\sigma_x}{\hat{E}}(1+\hat{\nu})\sin\theta\cos\theta + C_2; \qquad \beta = \frac{\sigma_x}{\hat{E}}(\sin^2\theta - \hat{\nu}\cos^2\theta) \tag{8,9}$$

Because the adhesive is constrained by the stiffer adherend at the adhesive–adherend interface, the displacement relations must satisfy Eq. (5, 6) at $\eta = \pm 1$ for a continuous interface to exist. Therefore, the boundary conditions to be satisfied at $\eta = \pm 1$ are:

$$\hat{U} = As \pm B; \qquad \hat{V} = \pm\beta - Ds \tag{10, 11}$$

ADHESIVE STRESS ANALYSIS

Based on earlier work,[3, 25, 26] the displacement functions for the adhesive in the (s), (η) and (z) directions, respectively, are assumed to be:

$$U = -f(s)(1-\eta^2) + As + B\eta \tag{12}$$

and

$$V = \varepsilon\eta - Ds; \qquad w = \Gamma z \tag{13, 14}$$

where:

$$\Gamma = \frac{-\hat{\nu}\sigma_x}{\hat{E}} \tag{15}$$

The terms A, B, and D are defined by Eq. (7 and 8).

The function $f(s)$ is to be determined by employing the stress equilibrium relations. It relates directly to the deformed shape of the adhesive when

constrained by the adherends under load for reasonable aspect ratios. The assumed forms for the displacements U and V, satisfy the boundary conditions, namely Eqs. (10) and (11) provided $\varepsilon = \beta$ at the adhesive–adherend interface. The displacements provide the normal strain relations

$$\varepsilon_s \equiv \frac{\partial U}{\partial s} = -f'(1-\eta^2)+A; \qquad \varepsilon_\eta \equiv \frac{\partial V}{\partial \eta} = \varepsilon \tag{16,17}$$

$$\varepsilon_z \equiv \frac{\partial w}{\partial z} = \Gamma; \qquad \gamma_{\eta s} = \frac{\partial U}{\partial \eta}+\frac{\partial V}{\partial s} = 2f\eta+R \tag{18,19}$$

where

$$R \equiv (B-D) \quad \text{and} \quad f' \equiv df/ds.$$

The stress equilibrium equations are satisfied on an average basis by their integration across the adhesive thickness. For the s-direction the ensuing plane strain relation is

$$\tfrac{1}{2}\int_{-1}^{1}\left[\frac{\partial \sigma_s}{\partial s}+\frac{\partial \tau_{\eta s}}{\partial \eta}\right]d\eta = 0 \tag{20}$$

Symmetry considerations require that σ_s and σ_η be even functions of (η) and that $\tau_{\eta s}$ be an odd function of (η). Furthermore, the average normal stresses will be denoted by

$$\bar{\sigma}_s = \tfrac{1}{2}\int_{-1}^{1}\sigma_s\, d\eta; \qquad \bar{\sigma}_\eta = \tfrac{1}{2}\int_{-1}^{1}\sigma_\eta\, d\eta \tag{21}$$

With this definition Eq. (20) reduces to

$$\frac{d\bar{\sigma}_s}{ds}+\tfrac{1}{2}\tau_{\eta s}\,|\,{}^{1}_{-1} = 0 \tag{22}$$

Similarly, the stress equilibrium relation in the η-direction,

$$\tfrac{1}{2}\int_{-1}^{1}\left[\frac{\partial \sigma_\eta}{\partial \eta}+\frac{\partial \tau_{\eta s}}{\partial s}\right]d\eta = 0 \tag{23}$$

is identically satisfied by symmetry considerations.

The averaged stresses $\bar{\sigma}_s$ and $\bar{\sigma}_\eta$ are obtained by substituting Eqs. (16–18) into the stress-strain relations and integrating over the adhesive thickness per Eq. (21). The ensuing averaged stress relations are:

$$\bar{\sigma}_s = \int_0^1 [\lambda v+2G\varepsilon_s]\, d\eta = -(\tfrac{2}{3}\lambda+\tfrac{4}{3}G)f'+(A+\varepsilon+\Gamma)\lambda+2GA \tag{24}$$

$$\bar{\sigma}_\eta = \int_0^1 [\lambda v+2G\varepsilon_\eta]\, d\eta = -\tfrac{2}{3}f'\lambda+(A+\varepsilon+\Gamma)\lambda+2G\varepsilon \tag{25}$$

$$\bar{\sigma}_z = \nu_a(\bar{\sigma}_s+\bar{\sigma}_\eta)-\frac{E_A\hat{\sigma}_x}{\hat{E}} \tag{26}$$

and;

$$\tau_{\eta s} = G\gamma_{\eta s} = G(2f\eta + R) \tag{27}$$

The governing differential equation whereby a solution to $f(s)$ is obtained, is formulated through substitution of Eqs. (19, 24 and 27) into Eq. (22). The ensuing governing differential equation is:

$$f'' - Mf = 0; \tag{28}$$

$$M \equiv \frac{3G}{\lambda + 2G} \tag{29}$$

The governing differential equation is a second order ordinary differential equation with constant coefficients. Since the shear stress $\tau_{\eta s}$ is an odd function of (η) the desired solution is:

$$f(s) = K \sinh(\sqrt{M}s) \tag{30}$$

The unknown constant (K) is determined by the physical requirement that

$$\bar{\sigma}_s(a/\sin\theta) = 0. \tag{31}$$

The resulting relationship is:

$$K = \frac{(A+\varepsilon+\Gamma)\lambda + 2GA^1}{(\tfrac{2}{3}\lambda + \tfrac{4}{3}G)\sqrt{M}\cosh(\sqrt{M}a/\sin\theta)} \tag{32}$$

Substitution of Eqs. (30) and (32) into the various adhesive deformation, (Eqs. 12–14) strain (Eqs. 16–19) and stress (Eqs. 24–27) relations gives the final form for these relations.

FORMULATION OF THE PROBLEM (CIRCULAR GEOMETRY)

The circular scarf joint geometry and the candidate notation $(\bar{s}, \bar{\eta}, \bar{\phi})$ are shown in Figure 3. Except for deletion of the plane strain condition, all assumptions are identical to that for the rectangular scarf joint. The adhesive disk is bonded between two deformable adherends at $\bar{\eta} = \pm 1$ and is two units thick. The disk is loaded in the $\bar{\eta}$-direction by a load $(P \sin\theta)$ which increases the adhesive thickness by 2ε and a shear load of $(P \cos\theta)$.

ADHESIVE STRESS ANALYSIS

The displacement boundary conditions at the adhesive–adherend interface are ascertained in a manner analogous to that for the rectangular geometry. Thus at $\bar{\eta} = \pm 1$, Eqs. (10) and (11) are valid. Moreover, Eq. (31) must also be satisfied.

The displacement functions for the adhesive in the $(\bar{s})$, $(\bar{\eta})$ and $(\bar{\phi})$ directions are identical in form to those defining U and V in Eqs. (12–13). The strains

corresponding to these displacements are identical to those defined in Eqs. (16, 17 and 19) for ε_s, ε_η and $\gamma_{\eta s}$, respectively. Moreover,

$$\varepsilon_{\bar{\varphi}} = \frac{U}{\bar{s}} = \frac{-f(1-\bar{\eta}^2)}{\bar{s}} + A + \frac{B\bar{\eta}}{\bar{s}} \tag{33}$$

The resulting averaged stress relations are:

$$\bar{\sigma}_{\bar{s}} = \bar{K} - \tfrac{4}{3}Gf' + 2GA \tag{34}$$

$$\bar{\sigma}_{\bar{\varphi}} = \bar{K} - \tfrac{4}{3}G\frac{f}{\bar{s}} + 2GA \tag{35}$$

$$\bar{\sigma}_{\bar{\eta}} = \bar{K} + 2G\varepsilon \tag{36}$$

where

$$\bar{K} = -\tfrac{2}{3}\lambda\left(\frac{f}{\bar{s}} + f'\right) + \lambda(2A + \varepsilon) \tag{37}$$

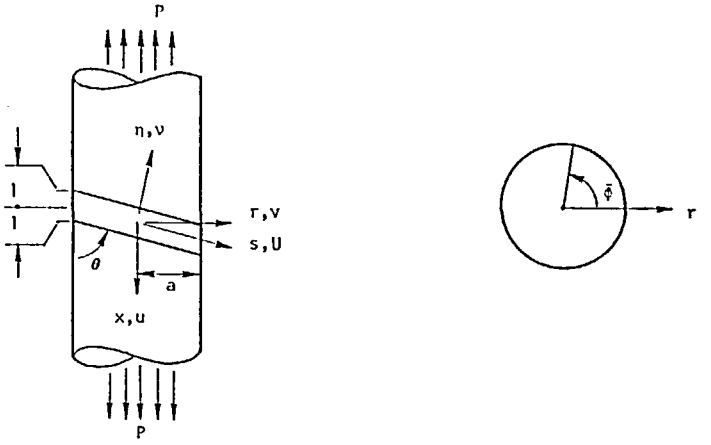

FIGURE 3 Circular scarf joint geometry.

The stress-equilibrium equations can be satisfied on an average basis by integration over the adhesive thickness. Integration of the equilibrium equation for the radial direction with respect to the $\bar{\eta}$-direction will determine $f(\bar{s})$ and the equation itself must vanish based on cylindrical coordinate equilibrium considerations. Thus:

$$\tfrac{1}{2}\int_{-1}^{1}\left(\frac{\partial\sigma_{\bar{s}}}{\partial_{\bar{s}}} + \frac{\partial\tau_{\bar{s}\bar{\eta}}}{\partial_{\bar{\eta}}} + \frac{\sigma_{\bar{s}} - \sigma_{\bar{\eta}}}{\bar{s}}\right) d\bar{\eta} = 0 \tag{38}$$

using the averaged stress definitions for $\sigma_{\bar{s}}$ and $\sigma_{\bar{\eta}}$. The governing differential equation, obtained is:

$$f'' + \frac{f'}{\bar{s}} - \left(\frac{1}{\bar{s}^2} + M\right) f = 0 \tag{39}$$

where $\tau_{\bar{s}\bar{\eta}}$ is an odd function of $\bar{\eta}$ due to symmetry about the $\bar{\eta} = 0$ plane. The equilibrium equation for the $\bar{\eta}$-direction is satisfied identically.

Equation (39) is a modified Bessel Equation of order one. A complete solution is of the form

$$f(\bar{s}) = \bar{A}I_1(\bar{s}\sqrt{\bar{M}}) + \bar{B}k_1(\bar{s}\sqrt{\bar{M}}) \tag{40}$$

where $I_1(\bar{s}\sqrt{\bar{M}})$ is a modified Bessel function of the first kind and $k_1(\bar{s}\sqrt{\bar{M}})$ is a modified Bessel function of the second kind.

As $\bar{s} \to 0$, U must be finite. This specifies that $f(\bar{s})$ be finite. Therefore $\bar{B} = 0$.

The constant $\bar{A}$ is determined using Eq. (31). Thus:

$$\bar{A} = \frac{-3\lambda(2A+\varepsilon)-6GA}{-2(\lambda+2G)\sqrt{\bar{M}}I_0\left(\frac{a\sqrt{\bar{M}}}{\sin\theta}\right)+\frac{4G}{a}I_1\left(\frac{a\sqrt{\bar{M}}}{\sin\theta}\right)\sin\theta} \tag{41}$$

Again, the final form for the various adhesive deformation, strain and stress relations is obtained using Eqs. (40) and (41) in an identical manner to that specified for the rectangular geometry.

BUTT JOINT ANALYSIS

For the limiting case whereby $\theta = 90°$, the solution for the butt joint is realized from the scarf joint analysis. The sole analytical difference is that the in-plane shear term previously identified by $(R) \to 0$ as θ approaches 90°. Therefore, the resulting shear strain is

$$\gamma_{\eta s} = 2\eta K \sinh(s\sqrt{\bar{M}}) \quad \text{(rectangular geometry)} \tag{42}$$

$$\gamma_{\bar{\eta}\bar{s}} = 2\bar{\eta}\bar{A}I_1(\bar{s}\sqrt{\bar{M}}) \quad \text{(circular geometry)} \tag{43}$$

This strain is a direct result of the material property discontinuity which exists at the adhesive–adherend interface. This readily substantiates that the scarf joint is nothing more than a butt joint with a transverse in-plane shear being superimposed on the adhesive.

VERIFICATION OF ANALYTICAL MODEL

The analytical accuracy of the present analysis, for the limiting case whereby the adherend modulus approaches infinity, has been verified by comparing it with the finite difference results of Ref. 3 (Figure 4). In turn, the results of Ref. 3 have been verified by the experimental data of Ref. 25 and by the energy methods approach of Ref. 26 and 28.

A singularity's region of influence is generally small compared to the distance to the nearest boundary. The region dominated by the stress singularity in Figure 4 and Ref. 3 is shown to be less than one adhesive thickness for the case of infinitely rigid adherends. While no appreciable growth in the region the singularity influences is anticipated, a numerical solution to evaluate the impact of the singularity for a finite adherend modulus is recommended.

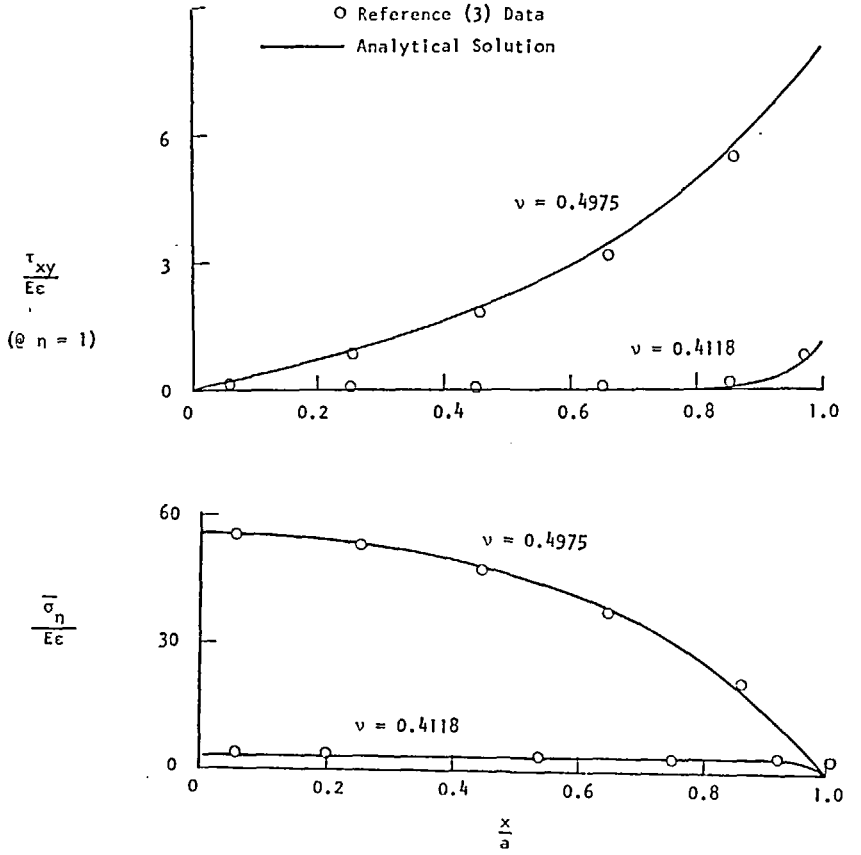

FIGURE 4 Comparison of axial stresses obtained from the two different methods of solution for circular geometry ($a = 10$, $\theta = 90°$).

OPTIMALLY DESIGNED TEST SPECIMENS

Employing the analytical methodology developed in the previous section, a parametric study was undertaken to ascertain the optimum geometry for

adhesive scarf and butt joint test specimens, whereby a uniform adhesive tensile and shear stress state (scarf joint only) exist over as large a segment of the half-span (a) as is practicable. This is accomplished by minimizing the adhesive–adherend discontinuity effect defined by $f(s)$ or $f(\bar{s})$. Figures 5–7

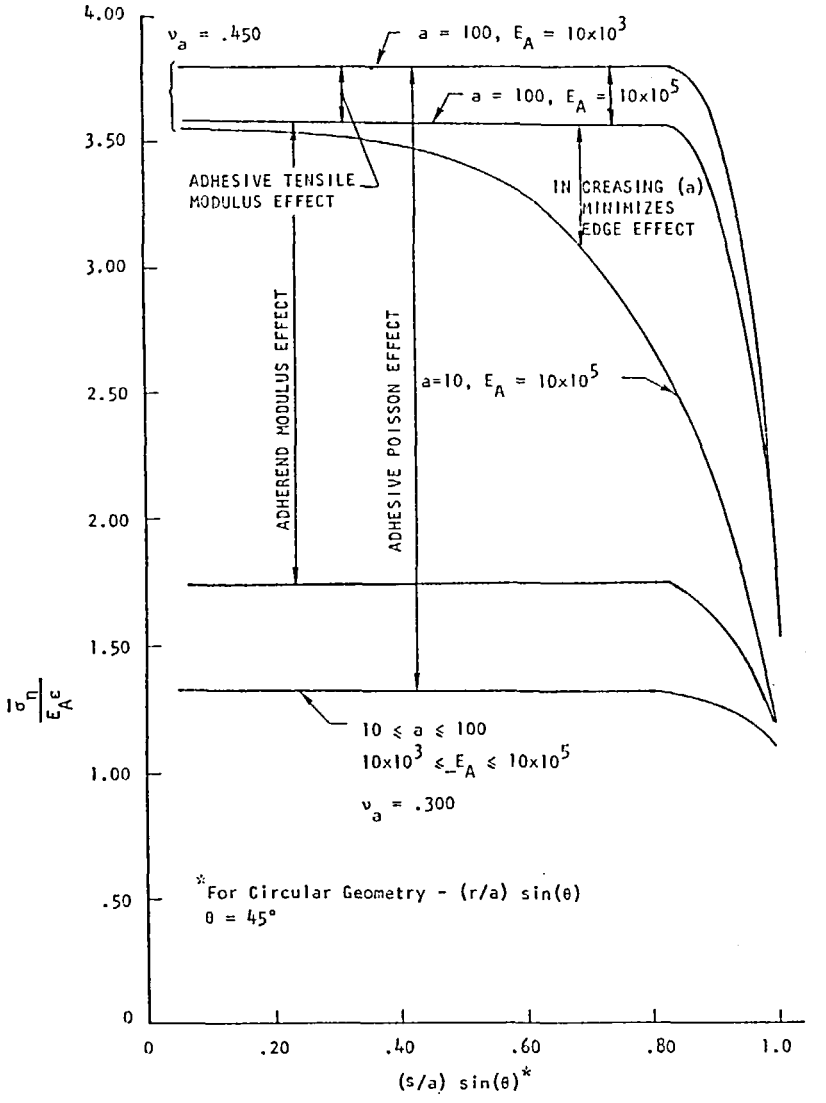

FIGURE 5 Primary normal stress distribution in rectangular or circular scarf (butt) joints ($\epsilon = 1.0$) aspect ratio ($10 \leqslant a \leqslant 100$).

determined from Eqs. (24–27 and 34–36) reveal that a uniform stress state can exist over 90–95% of (a). From such specimens, realistic "in situ" adhesive mechanical properties can be obtained. Moreover, Figures 5–7

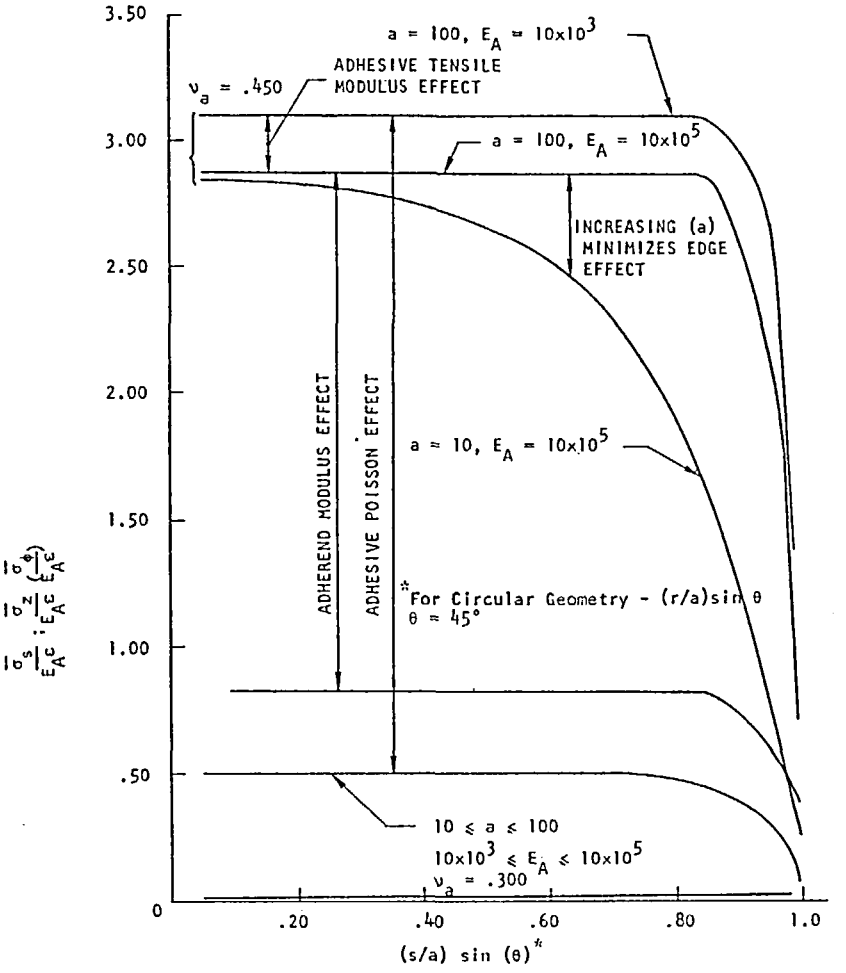

FIGURE 6 Shear stress distribution at adhesive-adherent interface in rectangular (circular) scarf (butt) joints ($\epsilon = 1.0$; $10\times10^3 \leqslant E_A \leqslant 10\times10^5$).

reveal that the pertinent variables are aspect ratio (a), the tensile modulus of the adhesive and the adherend (E_A and $\hat{E}$) and the Poisson's ratio (ν_a) of the adhesive. The data are normalized with respect to the adhesive's Young's modulus (E_A) and the displacement (ε) normal to the bondline.

Inspection of the figures reveals that it is the aspect ratio in combination with the Poisson's ratio of the adhesive which influences the spanwise uniformity (edge effect) of adhesive tensile and shear stresses. This edge effect is especially severe as the magnitude of the adhesive's Poisson's ratio approaches $\frac{1}{2}$. Additionally, the ratio of the adherend to the adhesive properties combine with the aspect ratio to dictate the magnitude of the normal and shear stresses in the adhesive for a given applied strain. In the limit case ($\hat{E} = E_A$) one attains the solution for a homogeneous, isotropic bar.

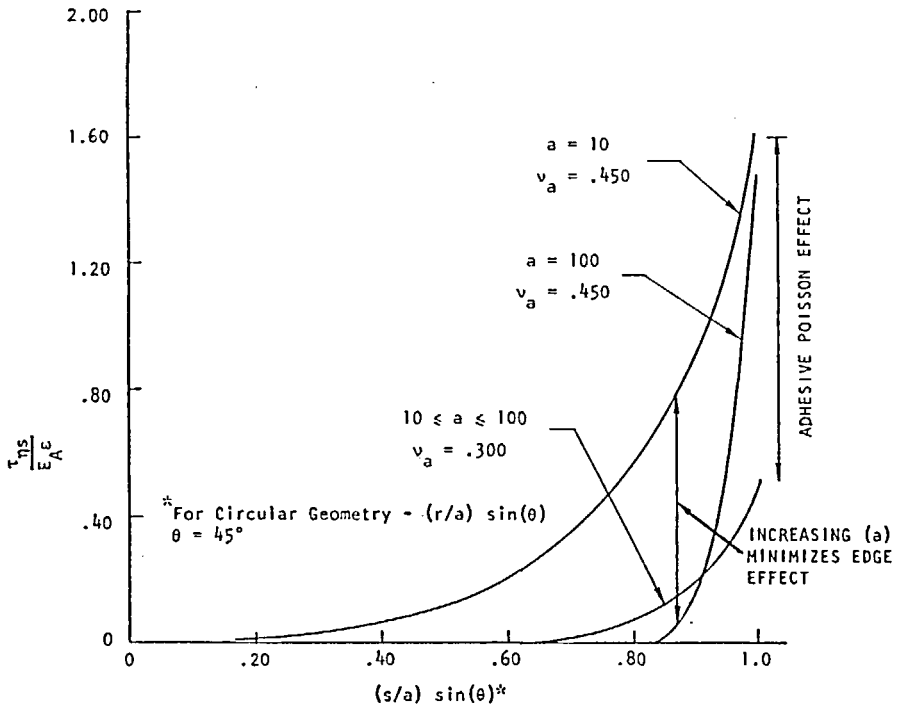

FIGURE 7 Shear stress distribution at adhesive-adherent interface in rectangular scarf (butt) joints. ($\varepsilon = 1.0$) aspect ratio ($10 \leqslant a \leqslant 100$).

In summary, by careful selection of the test specimen geometry one can obtain a near uniform triaxial stress state and impart to the adhesive a controlled shear stress. An aspect ratio of forty (up to 100 if the Poisson's ratio of the adhesive is $\geqslant 0.480$) is suggested to maintain the edge effect to within one or two adhesive thicknesses of the adhesive's free surface. As the mechanical properties obtained are average properties of the adhesive constrained between the much stiffer elastic adherends, this minor edge effect should not appreciably effect the test results. Thus, the uniformity of the

stress distribution over the bonded surface will enable one to obtain the mechanical linear and nonlinear viscoelastic response effects typical of adhesives at elevated load, temperature and moisture levels.

VISCOELASTIC EFFECTS

Under sufficiently high strain rates and/or elevated temperature and relative humidity levels, most adhesives will exhibit a viscoelastic response. The applicability of the scarf (butt) joint to attain meaningful viscoelastic response characteristics is possible by selection of a joint geometry within which the adhesive sees an approximately uniform stress state. Routine data reduction techniques[24, 29] are then used to obtain useful design data. This data can easily be used in conjunction with various viscoelastic analytical techniques to design "real structure". One such method is the "quasi-elastic" method, in which at time (t) the elastic moduli are replaced by corresponding viscoelastic relaxation moduli, resulting in the determination of the time dependent adhesive stress response of the component.

SUMMARY

An analytical methodology has been presented and its accuracy verified for the stress (strain) state in a thin adhesive layer bonded between linearly elastic adherends. Circular and rectangular geometries were analyzed for both scarf and butt joint configurations. Results presented point out the sensitivity of the adhesive stresses magnitude and spanwise uniformity to the geometrical dimensions of the test specimen and the adhesive and adherend's mechanical properties. The viscoelastic response of the adhesive can also be obtained using these properly designed scarf (butt) joint specimens.

Acknowledgement

This research was sponsored by the Air Force Materials Laboratory, Contract No. F33615-76-R-5205, with Dr. William Jones as program manager. The author also wishes to acknowledge the support received throughout this program from Dr. Richard Schapery.

List of Symbols

a	Specimen's half span (radius)
$A, \bar{A}, B, \bar{B}, D, K$	Constants
$C_i (i = 1 \rightarrow 4)$	Adherend rigid body displacement constants
$\hat{E}$	Young's modulus of adherend material
E_A	Young's modulus of the adhesive

L	Rectangular specimen's depth
P	Applied load
r	Radial coordinate of circular geometry
$\underline{s}, \underline{\eta}$	Rectangular coordinates parallel and perpendicular to adhesive bondline
$\bar{s}, \bar{\eta}, \bar{\phi}$	Cylindrical coordinates parallel, perpendicular and in the plane of the adhesive bondline
x, y, z	Rectangular coordinate system
u, v, w	Adherend displacements in x, y and z directions respectively
U, V	Adhesive displacements in s and η directions respectively
$\hat{U}, \hat{V}$	Adherend displacements in s and η directions respectively
ν	Dilatational strain
λ, G	Lame constants
$\hat{\nu}$	Poisson's ratio of adherend material
ν_a	Poisson's ratio of adhesive material
β	Normal adherend strain with respect to η axis
ε	Normal displacement of adhesive relative to center plane
$\hat{\varepsilon}_i$	Adherend normal strain with respect to x, y, z axes
ε_i	Adhesive normal strain
θ	Scarf joint angle
σ_i	Normal adhesive stress in the ith direction
$\bar{\sigma}_i$	Average adhesive normal stress in the ith direction
$\hat{\gamma}_{ij}$	Adherend shear strain in the ij direction
γ_{ij}	Adhesive shear strain in the ij direction
τ_{ij}	Adhesive shear stress in the ij direction

References

1. R. F. Zabora, "Adhesive Property Phenomena and Test Techniques," AD729873, July 1971.
2. Edward J. Hughes and John J. Rutherford, "Study of Micro-mechanical Properties of Adhesive Bonded Joints," Tech. Rep. 3744, Aerospace Research Center, General Precision Systems, Inc., Little Falls, NJ, August 1968.
3. G. H. Lindsey *et al.*, "The Triaxial Tension Failure of Viscoelastic Materials," Aerospace Research Laboratory Report 63-152, 1963.
4. Anon, "Solid Propellant Mechanical Behavior Manual," published by the Chemical Propulsion Information Agency, Publication No. 21, November 1963.
5. ASTM D-638, "Tensile Properties of Plastics". ASTM, Philadelphia.
6. N. A. DeBruyne and R. Houwink, *Adhesion and Adhesives* (Elsevier Publishing Co., Amsterdam, 1951).
7. G. M. Lehman and A. V. Hawley, "Investigation of Joints in Advanced Fibrous Composites for Aircraft Structures," Vol. 1, Air Force Flight Dynamics Laboratory-TR-69-43, June 1969.
8. G. C. Grimes *et al.*, "The Development of Nonlinear Analysis Methods for Bonded Joints in Advanced Filamentary Composite Structures," AD905201-L, Air Force Flight Dynamics Laboratory-TR-72-97, March 1972.
9. R. W. Gehring, T. T. Matoi and E. J. Hughes, "Evaluation of Environmental and Service Conditions on Filamentary Reinforced Composite Structural Joints and Attachments," Air Force Materials Laboratory-TR-71-194, Vol. 1, November 1971.
10. H. K. Shen and J. L. Rutherford, "Study of the Performance of Adhesive Bonded Joints," Singer-General Precision Co., Kearfott Division, Little Falls, N.J., Final Report, AD 880416, November 1970.
11. A. Marceau and W. M. Scardino, "Durability of Adhesive Bonded Joints," Air Force Materials Laboratory–TR–75–3, February 1975.

12. C. B. Norris, "Plastic Flow Throughout Volume of Thin Adhesive Bonds," Forest Products Laboratory Report No. 2092, March 1958.
13. J. J. Bikerman, *The Science of Adhesive Joints* (Academic Press, N.Y., 1961).
14. E. W. Kuenzi and G. H. Stevens, "Determination of Mechanical Properties of Adhesives For Use in the Design of Bonded Joints," Forest Products Laboratory Report No. FPL-011, September 1963.
15. R. W. Bryant and W. A. Dukes, "The Effect of Joint Design and Dimensions on Adhesive Strength," Explosives Research and Development Establishment, Report ERDE-5/M/68 (England) 1968.
16. W. T. McCarvill and J. P. Bell, *J. Adhesion* 6, 185–193 (1974).
17. J. L. Lubkin, *J. Appl. Mechanics* 24, 137 (1957).
18. Lackman *et al.*, "Advanced Composities Data for Aircraft Structural Design—Vol. III; Theoretical Methods," Air Force Materials Laboratory-TR-70-58, 1970.
19. ASTM E-229, "Shear Strength and Shear Modulus of Structural Adhesives". ASTM, Philadelphia.
20. R. L. Foye, "Inelastic Micromechanics of Curing Stresses in Composites," presented at ASME Annual Meeting, November 1975, Houston.
21. *Adhesion*, D. D. Eley, Ed. (Oxford Press, London, 1961).
22. C. J. Lin and J. P. Bell, *J. Appl. Polym. Sci. A*-1, 16, 1972.
23. W. J. Renton, "Structural Properties of Adhesives Quarterly Progress Report No. 3," Vought Advanced Technology Center, Air Force Materials Laboratory Contract No. F33615-76-R-5205.
24. W. J. Renton, "Structural Properties of Adhesives Quarterly Progress Report No. 5," Vought Advanced Technology Center, Air Force Materials Laboratory Contract No. F33615-76-R-5205.
25. A. N. Gent and P. B. Lindley, "The Compression of Bonded Rubber Blocks," Publication No. 324, Journal of British Rubber Producers Association, Volume 173, p. 111, 1959.
26. M. L. Williams and R. A. Schapery, "Studies of Viscoelastic Media," Aeronautical Research Laboratories Report No. ARL 62-366, June 1962.
27. R. A. Schapery, "Approximate Methods of Transform Inversion for Viscoelastic Stress Analysis," *Proc. Fourth U.S. National Congress of Appl. Mechanics*, 2, 1075 (1962).
28. M. L. Williams, P. J. Blatz and R. A. Schapery, "Fundamental Studies Relating to Systems Analysis of Solid Propellants," GALCIT SM61-5, California Institute of Technology, February 1961, ASTIA Report No. AD 256-905.
29. J. D. Ferry, *Viscoelastic Properties of Polymers*, 2nd Ed. (J. Wiley and Son, Inc., N.Y.).

MIDLAND MACROMOLECULAR MONOGRAPHS

A series of monographs based on special symposia held at the Midland Macromolecular Institute.
Editor: Hans-Georg Elias

Volume 4 MOLECULAR BASIS OF TRANSITIONS AND RELAXATIONS

Edited by Dale J. Meier

The fourth symposium held at the Midland Macromolecular Institute; co-sponsored by the Dow Chemical Company. On the 65th birthday of Raymond F. Boyer, it was decided to honor him by holding a symposium with the theme of molecular transitions, a field to which he has made such major scientific contributions. The symposium was organized broadly to cover the selected field, with invited speakers asked to present overviews of their topics, ranging from theory to mechanical and dielectric relaxational spectroscopy to relationships between molecular transitions and physical properties.

ISBN 0 677 11240 8 444pp January 1979

Volume 5 POLYMERIC DELIVERY SYSTEMS

Edited by Robert J. Kostelnik

This volume contains 18 papers presented at the fifth Midland Macromolecular Symposium POLYMERIC DELIVERY SYSTEMS held at the Midland Macromolecular Institute, Midland, Michigan. Because of the interdisciplinary nature of polymeric delivery systems, this volume should be of interest to polymer scientists, chemists, pharmacologists, chemical engineers, biologists and medical doctors.

ISBN 0 677 15940 4 320pp October 1978

Volume 6 FLOW-INDUCED CRYSTALLIZATION

Edited by Robert L. Miller

Crystallization in polymeric systems undergoing flow is of great importance to many commercial processes, e.g. fiber spinning (both melt and solution), hot drawing, film extrusion, and blow molding. Although we have a sound understanding and control of the crystallization process in quiescent melts (isotropic, isothermal systems), the more practical cases involving the transformation in non-isothermal and/or non-isotropic systems are extremely complicated. This book summarizes the status of knowledge and understanding of crystallization processes in flowing systems.

ISBN 0 677 12540 2 Approx 350pp March 1979

GORDON AND BREACH SCIENCE PUBLISHERS
41/42 William IV Street, London WC2
One Park Avenue, New York, NY 10016